

Trees and Matchings

Richard W. Kenyon	James G. Propp*	David B. Wilson
Laboratoire de Topologie	University of Wisconsin	Microsoft Research
Université Paris-Sud	Madison, Wisconsin	Redmond, Washington
kenyon@topo.math.u-psud.fr	propp@math.wisc.edu	dbwilson@alum.mit.edu

Submitted March 3, 1999; Accepted July 3, 1999

Abstract

In this article, Temperley’s bijection between spanning trees of the square grid on the one hand, and perfect matchings (also known as dimer coverings) of the square grid on the other, is extended to the setting of general planar directed (and undirected) graphs, where edges carry nonnegative weights that induce a weighting on the set of spanning trees. We show that the weighted, directed spanning trees (often called arborescences) of any planar graph G can be put into a one-to-one weight-preserving correspondence with the perfect matchings of a related planar graph \mathcal{H} .

One special case of this result is a bijection between perfect matchings of the hexagonal honeycomb lattice and directed spanning trees of a triangular lattice. Another special case gives a correspondence between perfect matchings of the “square-octagon” lattice and directed weighted spanning trees on a directed weighted version of the cartesian lattice.

In conjunction with results of Kenyon (1997b), our main theorem allows us to compute the measures of all cylinder events for random spanning trees on any (directed, weighted) planar graph. Conversely, in cases where the perfect matching model arises from a tree model, Wilson’s algorithm allows us to quickly generate random samples of perfect matchings.

1. Introduction

Temperley (1972) observed that asymptotically the $m \times n$ rectangular grid has about as many spanning trees as the $2m \times 2n$ rectangular grid has perfect matchings (dimer coverings). Soon afterwards he found a bijection between spanning trees of the $m \times n$ grid and perfect matchings in the $(2m + 1) \times (2n + 1)$ rectangular grid with a corner removed (Temperley, 1974). The second author of the present article and, independently, Burton and Pemantle (1993) generalized this bijection to map spanning trees of general (undirected unweighted) plane graphs to perfect matchings of a related graph. Here we extend this bijection to the directed weighted case.

*Supported by NSA grant MDA904-92-H-3060, NSF grant DMS 92-06374, and a grant from the MIT class of 1922.

This generalized bijection can be viewed as a way of “reducing” planar spanning tree systems to planar dimer systems (though not vice versa in general): for any graph whose spanning trees we are interested in, there is a related graph whose dimer coverings are in a natural one-to-one weight-preserving correspondence with the spanning trees of the original graph. Thus properties of spanning trees on any planar graph can be studied by considering the related dimer system. However, only certain dimer systems are related to spanning tree systems in the aforementioned way. Two important examples are perfect matchings of finite subgraphs of the hexagonal honeycomb lattice (combinatorially equivalent to “lozenge” tilings of finite regions; see e.g. Kuperberg (1994)) and perfect matchings of finite subgraphs of the “square-octagon” lattice. Both of these dimer models are in bijection with weighted, directed spanning trees on associated graphs.

There are a number of important applications of our bijection. Some questions about spanning tree models do not seem to be amenable to direct analysis, but can be approached if one first translates the problem into one involving the associated dimer model and then makes use of tools available in that context. Conversely, some problems involving dimers are most easily handled if one converts them into problems involving spanning trees (though this can be done only for a limited class of dimer models). We now describe these applications in greater detail.

One example of a spanning tree property that is easy to study after reducing the problem to that of dimers is the computation of certain probabilities, such as the probability that a directed edge e_1 is in the tree and the directed dual edge e_2 is in the dual tree. (For a definition of dual tree, see § 2.) The presence or absence of the dual edge e_2 in the dual tree is not a local event with respect to the (primal) tree model; that is, the event is not determined by the presence or absence of a fixed set of edges in the primal tree. (The fact that e_2 is an *oriented* edge is crucial here.) On the other hand, the event in question is a local event in the associated matching process, since the matching directly incorporates both primal and dual directed trees. The probabilities of local events in either the tree or matching model are easy to compute (Burton and Pemantle (1993), Kenyon (1997b)), but events of the above type are harder if not impossible to compute from the point of view of the tree only (Burton and Pemantle, 1993).

Another spanning tree property that can be studied via dimers is the number of times that the path connecting two points in a spanning tree winds around the two points. In § 5 we relate these winding numbers to height functions in the dimer model; the first author has shown in Kenyon (1997b) how to compute properties of these height functions (and consequently the corresponding winding numbers) such as the variance.

Dimer systems can also be studied via trees, if the given dimer system has a spanning tree model associated with it. For instance, one can sometimes enumerate the dimer coverings of a graph by counting the number of spanning trees in the associated tree model. In § 6 we show a variety of such graphs, together with exact formulas for the number of dimer coverings, where the easiest (or only) way we know to obtain these formulas is to count spanning trees. In the dimer model on a bounded region, the boundary can have an important (long-range) effect on the number of configurations (Cohn et al., 1998). In this case the regions which arise from the associated spanning

tree process give the most “natural” boundary conditions for the dimer model, in the sense that the boundary has the least long-range influence (Kenyon, 1997a).

Another case where a spanning tree model is useful for studying the associated dimer model is in the generation of random samples. Wilson’s algorithm (Propp and Wilson, 1998) can be used to generate random spanning trees quickly — the expected running time is given by the sum of two mean hitting times. For the lattice of octagons and squares, the expected running time is *linear* in the number of vertices. For the usual lattice of squares, when a rectangular region has moderate aspect ratio, the running time is nearly linear, but with a logarithmic correction factor.

Finally, Burton and Pemantle (1993) prove that the uniform measure on spanning trees of the $n \times n$ square grid converges as $n \rightarrow \infty$ to the unique translation-invariant measure of maximal entropy on the set of spanning forests with no finite component. Consequently the associated dimer model (on \mathbb{Z}^2) has a unique translation-invariant measure of maximal entropy. We do not know how to prove this directly from the dimer model itself, or in any other dimer model except those arising from our construction via a bijection with *undirected* (but possibly weighted) spanning trees.

We remark that other combinatorial systems that can also be reduced to dimer systems in a similarly simple way include the Ising model on planar graphs (Fisher, 1966) and systems of non-intersecting lattice paths (Lindström, 1973; Gessel and Viennot, 1989).

In § 2 we prove the generalized version of Temperley’s bijection. In the two succeeding sections (§§ 3-4) we illustrate the bijection with two examples: In § 3 we exhibit a bijection between directed spanning trees on the triangular lattice and perfect matchings of the hexagonal honeycomb lattice. Our bijection cannot be applied directly to matchings on the square-octagon lattice, but in § 4 we show how to locally transform this lattice so that the bijection can be applied. This transformation enables the rapid generation of random dimer configurations of the square-octagon lattice. Then in § 5 we show how the winding number of arcs in a spanning tree can be related to the height function on the corresponding perfect matching. In § 6 we use our generalized bijection to compute the exact number of perfect matchings of some “locally symmetric” finite planar graphs, that is, graphs that arise as finite induced subgraphs of highly symmetric infinite planar graphs. Lastly, in § 7 we give some open problems.

2. Generalized Temperley Bijection

Let G be a finite connected directed graph embedded in the plane, with multiple edges and self-loops allowed. In general the edges of G will be weighted, that is, each directed edge from vertex u to vertex v has a nonnegative weight assigned to it, which need not be the same as the weight of other directed edges from u to v or from v to u . Undirected graphs can be fit into our framework by thinking of each undirected edge as two directed edges, one in each direction, embedded in the plane so as to coincide. (We will discuss issues related to choice of embedding at the end of this section.) Unweighted graphs can be fit into our framework by assigning each edge weight 1.

By a **directed spanning tree** (or **arborescence**) T of G we mean a connected, contractible union of (directed) edges such that each vertex of G except one has exactly one outgoing edge in T . Note that the exceptional vertex necessarily has no outgoing edges in T ; it is called the **root** of T . We define the **weight** of such a tree T to be the product of the weights of its edges.

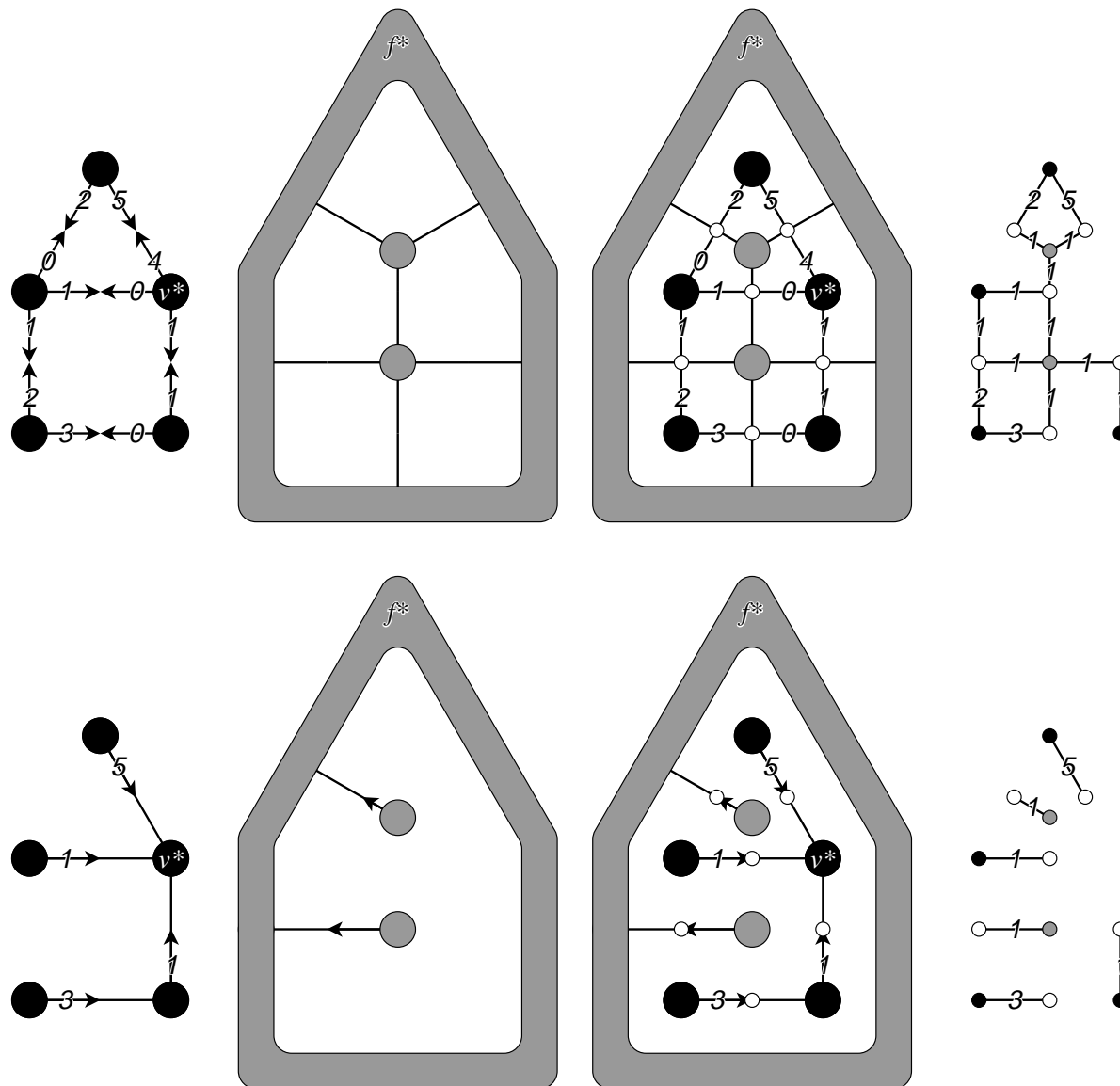


Figure 1: Illustration of the generalized Temperley bijection.

We will make a new weighted graph $\mathcal{H}(G)$ based on G , as shown in the top half of Figure 1. G is shown in the top left-most panel. G^\perp , the dual graph of G (second panel), has vertices, edges, and faces of G^\perp corresponding to faces, edges, and vertices of G , respectively (including a vertex, here marked f^* , that corresponds to the unbounded,

external face of G , and is represented in “extended form”, i.e., as a spread-out region rather than a small dot). We can embed G and G^\perp simultaneously in the plane, such that an edge e of G crosses the corresponding dual edge e^\perp of G^\perp exactly once and crosses no other edge of G^\perp . If we introduce a new vertex at each such crossing, we get the graph shown in the third panel. This is the graph $\mathcal{H}(G)$. Pictorially, we may derive $\mathcal{H}(G)$ from G by adding a new node on each edge e and a new node on each face f and joining them by a new edge if e is part of the boundary of f . To avoid confusion, we will say that $\mathcal{H}(G)$ has nodes and links whereas G has vertices and edges.

Here is an alternative, direct definition of $\mathcal{H}(G)$ that does not go by way of the dual graph. Put $V =$ the set of vertices of G , $E =$ the set of edges, $F =$ the set of faces (including the unbounded face). Define $\mathcal{H}(G)$ as the weighted undirected graph with a node \bar{v} corresponding to each vertex v of G , a node \bar{e} corresponding to each edge e of G , and a node \bar{f} corresponding to each face f of G , with a link joining two nodes in $\mathcal{H}(G)$ if the corresponding structures in G are either an edge and one of its endpoints *or* an edge and one of the faces it bounds.

The weight of a link between a vertex-node \bar{v} and an edge-node \bar{e} (where v is an endpoint of e in G) is the weight of edge e in G directed away from v . The weight of a link between a face-node \bar{f} and an edge-node \bar{e} (where e bounds face f in G) is always 1.

A **perfect matching** of a graph H is a collection of edges M such that each vertex is a vertex of exactly one edge of M . The **weight** of a perfect matching is the product of the weights of its edges (1 by default in the unweighted case).

In the case of both trees and matchings, the weighting gives rise to a probability distribution on the objects in question, in which the probability of any particular object (tree or matching) is proportional to its weight.

Let v^* be a vertex of G and f^* a face of G , and let $\mathcal{H} = \mathcal{H}(v^*, f^*)$ be the induced subgraph of $\mathcal{H}(G)$ obtained by deleting the nodes \bar{v}^*, \bar{f}^* (along with all incident edges in $\mathcal{H}(G)$), as shown in the fourth panel of the top half of Figure 1). Since by Euler’s formula $(|V| - 1) + (|F| - 1) = |E|$, $\mathcal{H}(v^*, f^*)$ is a balanced bipartite graph, so it may have perfect matchings. (For a nice tree-based proof of Euler’s formula, see (Aigner and Ziegler, 1998, page 57).)

Theorem 1 *If v^* is incident with f^* , then there is a weight-preserving bijection between spanning trees of G rooted at v^* and perfect matchings of $\mathcal{H}(v^*, f^*)$. If v^* is not incident with f^* , there remains a weight-preserving injection from the spanning trees of G rooted at v^* to the perfect matchings of $\mathcal{H}(v^*, f^*)$.*

This theorem, along with its proof, is a generalization of a result of Temperley (1974) which is discussed in problem 4.30 of (Lovász, 1979, pages 34, 104, 243–244). The unweighted undirected generalization was independently discovered by Burton and Pemantle (1993), who applied it to infinite graphs, and also by F. Y. Wu, who included it in lecture notes for a course.

Note that in the special case when we take all weights of G to be 1, the first part of the theorem implies that the number of perfect matchings of $\mathcal{H}(v^*, f^*)$ is independent of v^* and f^* , provided that v^* and f^* are incident with one another.

Henceforth, we refer to perfect matchings as simply “matchings,” and directed spanning trees of G rooted at v^* as simply “spanning trees” or occasionally just “trees.”

PROOF OF THEOREM: It will be enough to exhibit a weight-preserving injective mapping from the set of spanning trees of G into the set of matchings of $\mathcal{H}(v^*, f^*)$, and to show that when v^* is incident with f^* , every matching of $\mathcal{H}(v^*, f^*)$ arises from a spanning tree of G .

Given a spanning tree T of G rooted at V^* , the set of edges of G^\perp that do not cross edges of T form a spanning tree of G^\perp , called the **dual tree** and here denoted by T^\perp . Orient the edges of T^\perp so that they point towards f^* . Then a matching M of $\mathcal{H}(v^*, f^*)$ can be obtained as shown in the bottom half of Figure 1. Specifically, for each $v \in V$, pair \bar{v} with the unique \bar{e} such that v is an endpoint of e and e is pointing away from v in the orientation of T , and for each $f \in F$, pair \bar{f} with the unique \bar{e} such that e bounds f and e^\perp is pointing away from f in the orientation of T^\perp . The left panel shows the tree T ; the second panel shows the dual tree T^\perp ; the third panel shows both trees; and the fourth panel shows the matching M , which has the same weight as T .

To verify that this construction always gives a matching M of $\mathcal{H}(v^*, f^*)$, it suffices to show that no edge-node \bar{e} is paired twice. But this could only happen if we had $e \in T$ and $e^\perp \in T^\perp$, contradicting the definition of a dual tree.

From the matching M we can easily recover T as the set of edges e such that \bar{e} is paired with a vertex-node in $\mathcal{H}(v^*, f^*)$ under the matching M . Hence the mapping $T \mapsto M$ is injective.

Now suppose v^* is incident with f^* , and let M be a matching of $\mathcal{H}(v^*, f^*)$. Let \tilde{T} be the set of edges e of G such that \bar{e} is paired with a vertex-node by M . To complete the proof of the theorem, we must show that \tilde{T} is a spanning tree. Note that \tilde{T} has $|V| - 1$ edges, so it suffices to prove that \tilde{T} is acyclic.

Suppose \tilde{T} contained a cycle C , say of length n . C divides the plane into two (open) regions, one of which contains both v^* and f^* and the other of which contains neither. We claim that each part contains an odd number of nodes of $\mathcal{H}(G)$ and hence an odd number of nodes of the subgraph $\mathcal{H}(v^*, f^*)$ as well. For, suppose we modify G by replacing either of the two regions by a single face. By Euler’s formula, the number of vertices, edges, and faces in the resulting graph must be even. Since there are an even number of these elements on the cycle C (n vertices and n edges) and an odd number in the modified region (1 face), the unmodified region must have an odd number of elements as well.

Since the edges of C disconnect $\mathcal{H}(v^*, f^*)$ into parts lying in the two regions, M must match each region within itself. But this is impossible, since each region has been shown to contain an odd number of nodes of $\mathcal{H}(v^*, f^*)$. This completes the proof of the theorem. \square

As was remarked earlier, the theorem implies that when v' is incident with f' and v'' is incident with f'' , the matchings M' of $\mathcal{H}(v', f')$ are equinumerous with the matchings M'' of $\mathcal{H}(v'', f'')$; in fact, the proof of the theorem provides a bijection between the two sets of matchings. This bijection can be understood without reference to spanning trees, as a process of “sliding edges.” Specifically, one iteratively defines a chain $v'' = v_0, e_0, v_1, e_1, v_2, \dots$ such that, for all i , \bar{e}_i is the node that M' pairs with \bar{v}_i and v_{i+1} is the vertex of e_i that is distinct from v_i . This chain cannot repeat any vertices, since any closed loop would encircle an odd number of nodes (see the preceding proof), so it must terminate by arriving at v' after some number of steps. That is, the chain must be of the form

$$v'' = v_0, e_0, v_1, e_1, v_2, \dots, e_{r-1}, v_r = v'$$

for some r . Once one has found such a chain, one modifies the matching M' by pairing \bar{e}_i with \bar{v}_{i+1} instead of \bar{v}_i . One then does the same with a chain of dual-edges joining the faces f'' and f' , obtaining the desired matching M'' .

We also remark that in addition to one’s having a choice of which vertex-node and face-node to delete, one often has a choice of how to embed a graph in the plane in the first place. For instance, in the case where G has a single edge from u to v and a single edge from v to u , we allowed the two edges to be embedded so as to coincide. What if we had required the embedding to be proper, so that the two edges could meet only at their endpoints? Then one would get a slightly enlarged graph $\mathcal{H}(G)$ in which a single edge-node in the original $\mathcal{H}(G)$ was replaced by two edge-nodes and a face-node in between (corresponding to the digon bounded by the two edges). It is easy to see in this case that perfect matchings of the first $\mathcal{H}(G; v^*, f^*)$ are in bijection with perfect matchings of the second $\mathcal{H}(G; v^*, f^*)$. When there are multiple directed edges in each direction, the number of possible embeddings increases rapidly; but our main bijection theorem guarantees that the number of matchings of $\mathcal{H}(G; v^*, f^*)$ is insensitive to the choice of embedding.

Moreover, having several directed edges from v to w is in a certain sense equivalent to having a single edge from v to w whose weight is the sum of the weights of those directed edges. It is not true that the spanning trees of the former graph are in bijection with those of the latter graph; however, there is an obvious mapping from the former to the latter, and this correspondence is weight-preserving, in the sense that the weight of a spanning tree of the smaller graph is the sum of the weights of the spanning trees in the larger graph to which it corresponds. It follows that the sum of the weights of all the spanning trees is the same for both graphs.

Given a graph H , it can be an amusing problem to find a directed graph G such that $\mathcal{H}(G; v^*, f^*) = H$. We leave it to the reader to show that this cannot be done with the square-octagon lattice of Figure 3. (That is, there is a finite subgraph of the lattice, such that any subregion H of the square-octagon lattice containing this subgraph will fail to be of the form $\mathcal{H}(G; v^*, f^*)$.)

3. The Hexagonal Lattice

In this section we illustrate the technique of Theorem 1 by giving a bijection between spanning trees of a directed graph and matchings in the hexagonal (honeycomb) lattice.

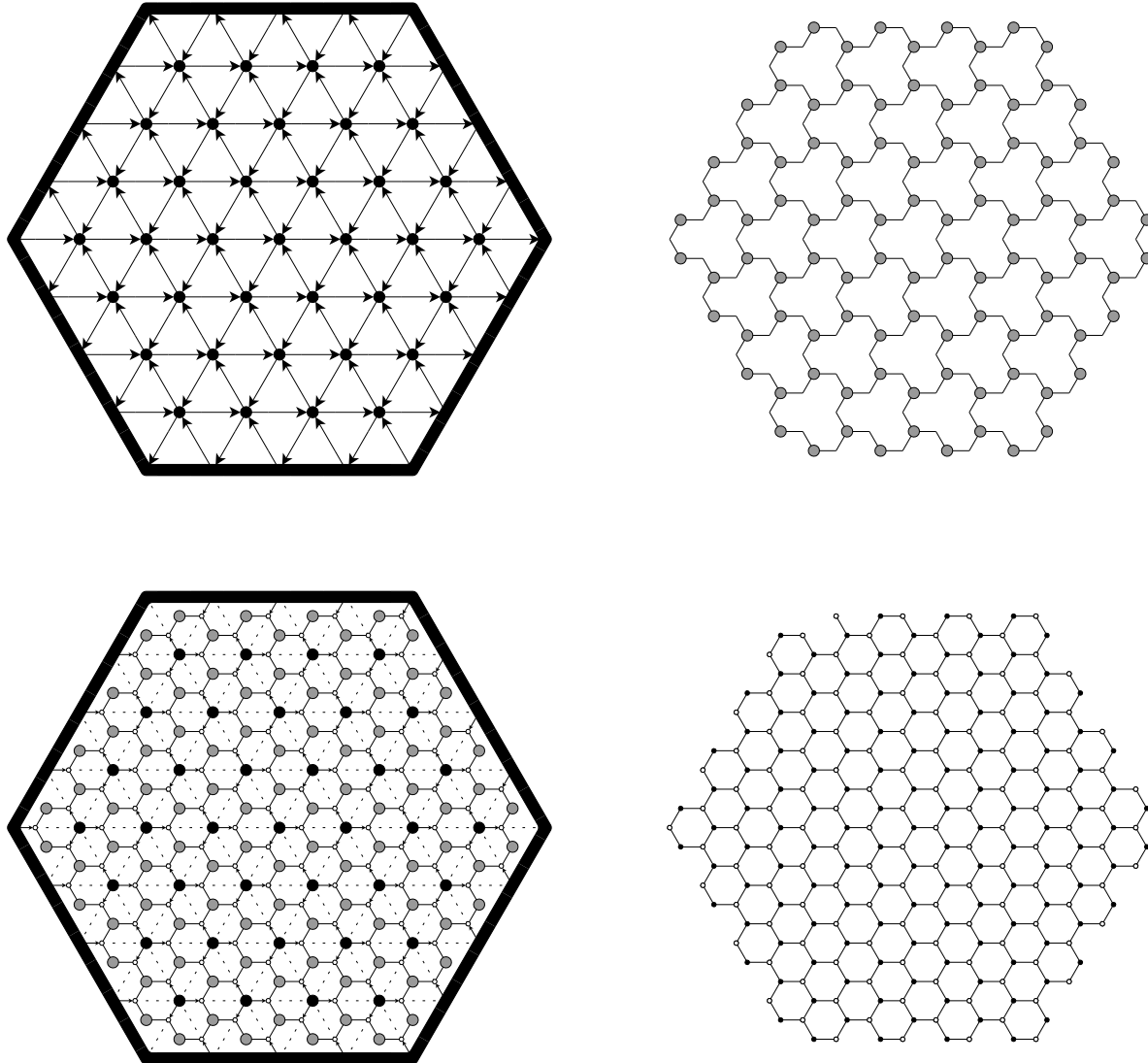


Figure 2: Generalized Temperley bijection for the hexagonal lattice.

Panel (a) of Figure 2 contains the plane graph G , a directed triangular lattice. (Here and throughout the rest of the article, the upper-left, upper-right, lower-left, and lower-right panels of a four-panel figure will be denoted by (a), (b), (c), and (d), respectively.) G contains an “outer vertex” which is represented in extended form, in this case drawn as a large hexagon. In the examples throughout the rest of the article, either G or G^\perp (or both) will have an outer vertex that is drawn in extended form. Panel (b) shows the dual of G , a hexagonal lattice. The edges in panel (b) have been drawn bent slightly

so that the union of G and its dual (panel (c)) can be recognized as a subset of the hexagonal lattice. The dotted edges in panel (c) have weight zero, and may be omitted; they are shown only to highlight the connection with panel (a). The graph $\mathcal{H}(G)$ can be read off from panel (c); it is a hexagonal lattice with about three times as many hexagons as G^\perp . Panel (d) shows the graph $\mathcal{H}(v^*, f^*)$, which is obtained from $\mathcal{H}(G)$ by removing v^* (the outer vertex of G) and f^* (the leftmost vertex at the top of G^\perp). We shall apply this correspondence in § 6.9.

4. The Square-Octagon Lattice

Here we illustrate a less direct application of Theorem 1, and give a bijection between perfect matchings of certain planar graphs and spanning trees on an associated graph. Consider perfect matchings on the square-octagon lattice, an excerpt of which is shown in Figure 3. This graph does not arise as $\mathcal{H}(G)$ for any graph G , so Theorem 1 does not apply immediately. Nonetheless, it is possible to generalize the bijection to apply

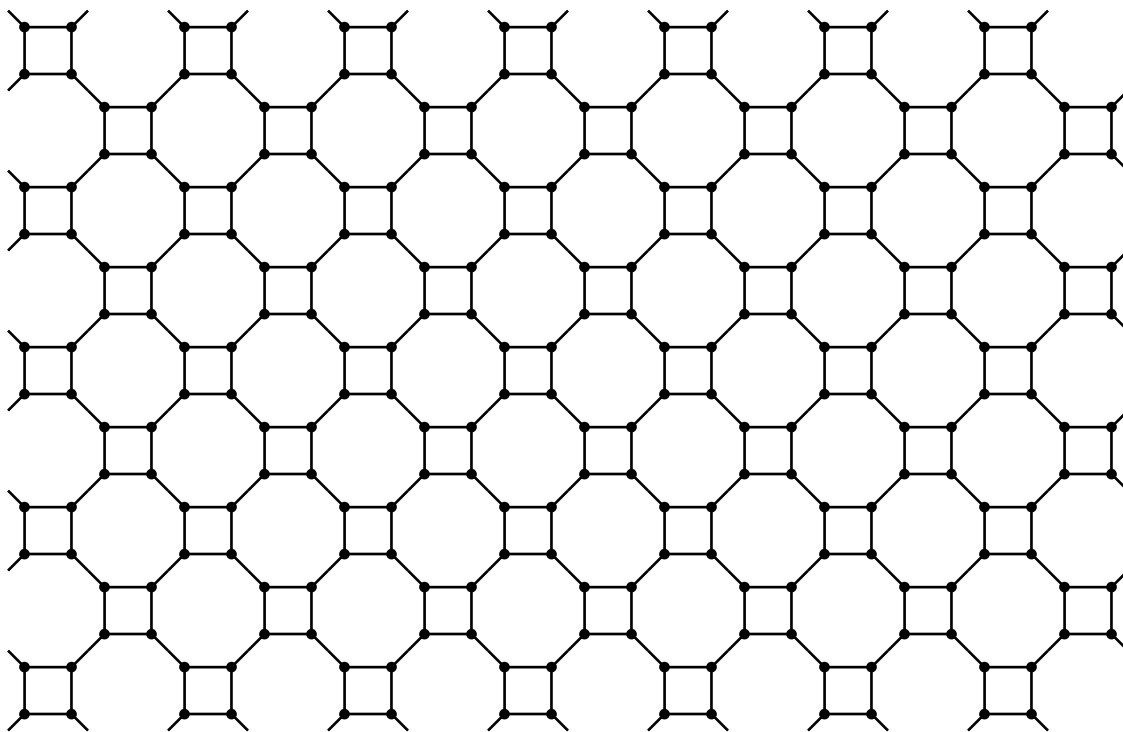


Figure 3: A portion of the square-octagon lattice.

to this lattice. To do it we need to apply two transformations to the lattice. The first transformation is called “urban renewal,” a term coined by the second author, who learned of the method from Greg Kuperberg. In the second transformation, we adjust the edge weights. At that point, if a square-octagon region has suitable boundary conditions, the transformed graph can be expressed as $\mathcal{H}(G)$ for some graph G .

4.1. Urban renewal

Tricks such as urban renewal have been used by researchers in the statistical mechanics literature for decades, but since understanding it is essential for what follows, a description is included here of the special case of urban renewal that we will need. One views the square-octagon lattice as a set of cities (the squares) that communicate with one another via the edges that separate octagons. Now the graph of cities (with each city being thought of as adjacent to the four closest cities) is itself bipartite, so we may say that every city is either rich or poor, with every poor city having four rich neighbors and vice versa. The process of urban renewal on a poor city merges each of its four vertices with its four neighboring vertices, and then changes the weights of the edges of the poor city from 1 to $1/2$, as shown in Figure 4. We will show that the sum of the weights of the matchings in the “before” graph is twice the sum of the weights of the matchings in the “after” graph. We will do this by associating with each matching in the before graph one or two matchings in the after graph, and vice versa. More precisely, we divide the set of matchings in the before graph into equivalence classes of size 1 or 2, and likewise with the set of matchings of the after graph, and we create a bijection between these equivalence classes so that the weight of each class in the before graph (that is, the sum of the weights of the matchings that constitute that class) is twice the weight of the associated class in the after graph.

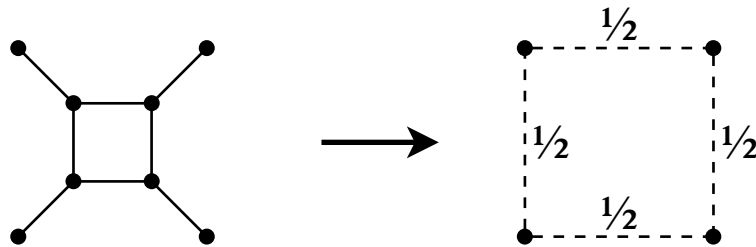


Figure 4: Urban renewal. The poor city is the inner square in the left graph, and is connected to the rest of the graph (not shown) via only four vertices at the corners, some of which may actually be absent. The city and its connections are replaced with weight $1/2$ edges, shown as dashed lines. All other edges have weight 1.

Matchings in the “before” graph get mapped via urban renewal to matchings in the “after” graph by deleting the four vertices of the poor city and its incident edges, and then pairing up any resulting unpaired vertices. Prior to urban renewal, every matching will match k of the poor city’s vertices with the rest of the graph, with k equal to 0, 2, or 4; if $k = 2$, then these vertices are adjacent. If $k = 0$, then since the city has two possible matchings, a pair of matchings in the “before” graph get mapped to one matching (of half their combined weight) in the “after” graph. If $k = 2$ (two of the poor city’s vertices match to each other and two match outward), then the matching in the before graph gets mapped to a matching in the after graph that uses one weight- $1/2$ edge. The matchings with $k = 4$ get mapped to a pair of matchings in the after

graph, each using two weight- $1/2$ edges. Thus urban renewal on a poor city will reduce the weighted sum of matchings by a factor of $1/2$. (If one is trying to generate random matchings rather than merely count them, then, given a random bit, a random matching in the before graph is readily transformed into a random matching in the after graph, and conversely, given a random bit, a random matching in the after graph is readily transformed into a random matching in the before graph.)

The preceding discussion applies to cities in the interior of a finite subgraph of the infinite square-octagon grid. Along the boundaries, some of the poor cities may not have four neighbors, but urban renewal can still be done. One way to see this is to adjoin a pair of connected vertices to the graph for each missing poor city's neighbor, and connect one of these vertices to the poor city. This operation won't affect the number of matchings or their weights, and after urban renewal, the pair may be deleted again, again without affecting the matchings — so if some of the poor city's vertices don't have neighbors, these vertices are deleted by urban renewal.

Doing urban renewal on each of the poor cities in the square-octagon lattice will yield the more familiar Cartesian lattice.

4.2. Weighted directed spanning trees

Consider the finite square-octagon graph shown in Figure 5. It has 3 octagonal bumps on the left, and four on top, so by convention let's call it a region of order $3, 4$. (In a region of order L, M , there are $2LM$ octagons.) An octagonal column and octagonal row meet at a unique square; these will be the rich cities. The rich cities have been labeled by their coordinates to enhance clarity. The other $(L + 1)(M + 1)$ squares will be the poor cities, and we will do urban renewal on them as shown in Figure 5. We will compute the weighted number of matchings of the resulting graph, and multiply by $2^{(L+1)(M+1)}$.

Now for any vertex, we may re-weight all the edges incident to the vertex (multiplying them all by the same constant) without affecting the probability distribution on matchings: this has the effect of multiplying the weight of any matching by that same constant. Re-weight the edges as follows: for the rich city (complete or incomplete) with coordinates i, j ($0 \leq i \leq M$, $0 \leq j \leq N$), multiply the weights of the edges incident to the top left and lower right corners by 2^{-i-j} , the other two corners by 2^{i+j} .

Edges that are internal to the rich cities remain weighted by $2^{i+j}2^{-i-j} = 1$. The long edges come in pairs. The lower or right edge of the pair gets its weight doubled, to become 1, while the upper or left edges of the pair gets its weight halved to become $1/4$.

The next thing we need to do is interpret this graph as a plane graph and its dual (see Figure 6). The upper left vertices of the small squares represent vertices, the lower right vertices represent faces, and the other two vertices represent edges. The result is the graph F shown in Figure 6, which has $LM + 1$ vertices — LM of them on a grid, and one “outer vertex” (not in the original graph) that all the open edges connect to. A random spanning tree on the vertices of this graph rooted at the outer vertex determines a dual tree on the faces of this graph, rooted at the upper left face, and the two together

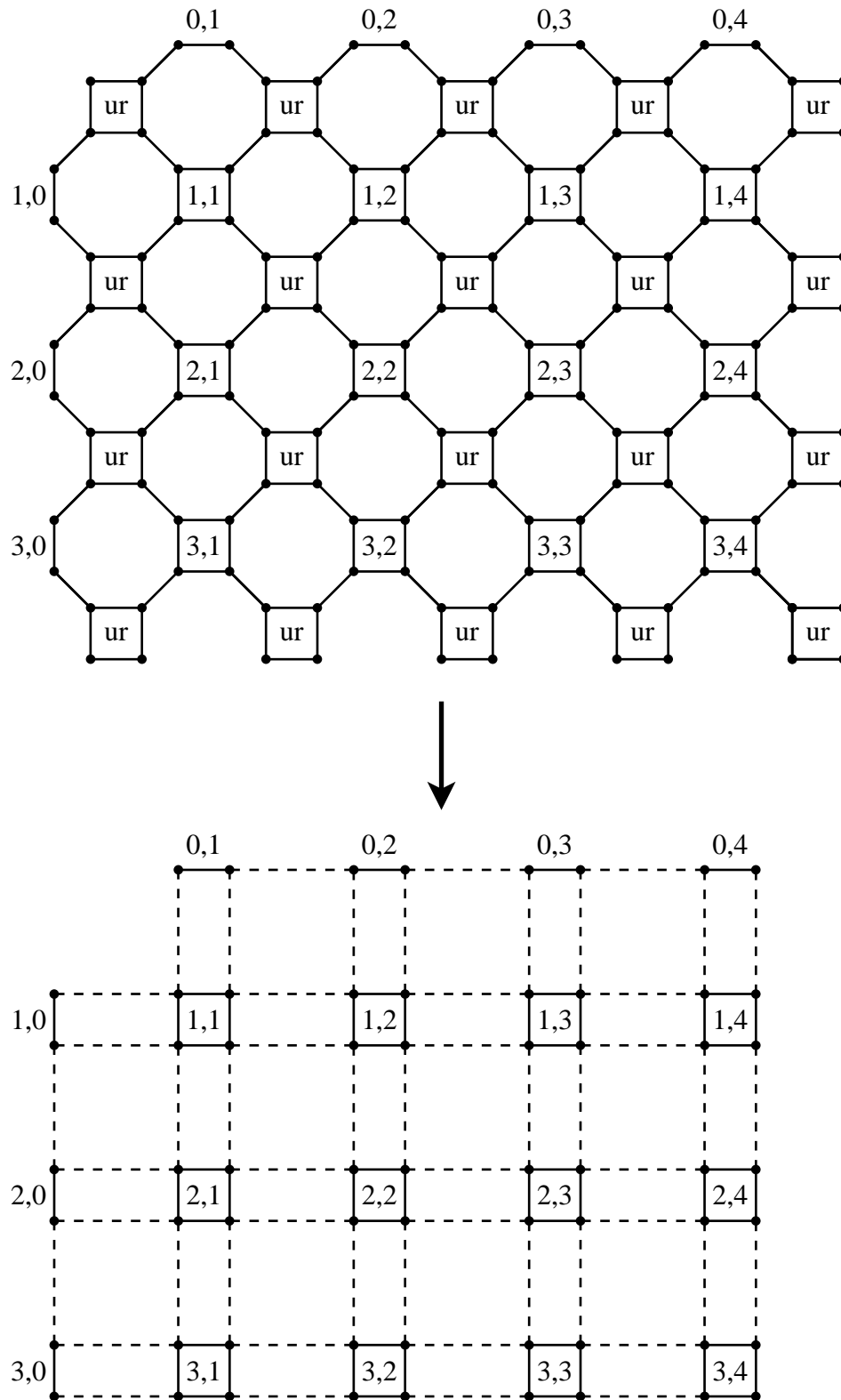


Figure 5: Region of order 3,4 before and after urban renewal. The poor cities on which urban renewal is done are labeled with “ur,” the rich cities are labeled with their coordinates. Dashed edges have weight $1/2$.

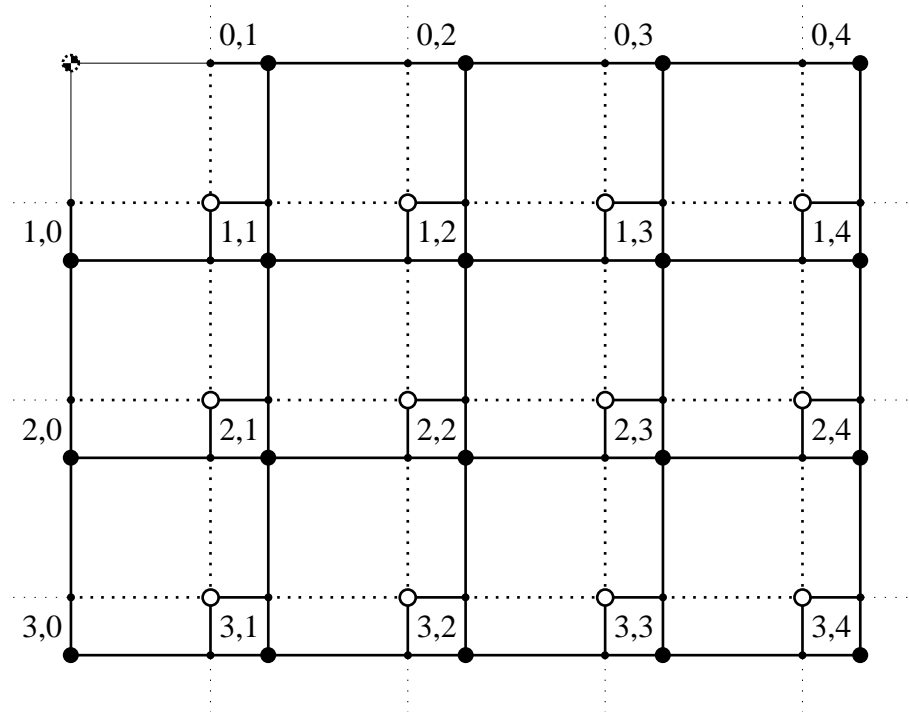


Figure 6: The region from Figure 5 after re-weighting. Dashed edges have weight $1/4$. A distinguished vertex and distinguished outer face have been adjoined to give a graph H which nicely decomposes into a graph G and a weighted directed graph F .

determine a matching of the graph in Figure 5. The weight of the matching equals the weight of the primal tree, since the re-weighting left every dual tree with weight one.

4.3. Random generation in linear expected time

Using the loop-erased random-walk spanning tree generator (Propp and Wilson, 1998), and the bijection derived above between spanning trees of a weighted graph and matchings of the square-octagon regions, we can sample random matchings in linear time. The tree generator builds the tree by doing a sequence of loop-erased random walks on the underlying graph. (From any vertex v , the probability of moving to a particular neighboring vertex w is proportional to the weight of the edge from v to w ; this determines a random walk on the graph. For details on loop-erasure, see (Propp and Wilson, 1998).) It has been shown that the expected running time (or rather, number of random-walk steps) of the tree algorithm is given precisely by

$$\sum_v E \left[\begin{array}{l} \# \text{ times a that random walk started} \\ \text{at } v \text{ visits } v \text{ before hitting the root} \end{array} \right].$$

For our random walk, the moves are right or down with probability $4/10$ and up or left with probability $1/10$, since in the face graph the links going to the left or up have

1/4 the weight of the other links. For large graphs, the random walk drifts to the right and down, so we consider this biased random walk on \mathbb{Z}^2 . Starting at the origin, with probability 1 the origin is visited finitely many times. Let R be the expected number of times the random walk returns to its starting location, counting the “return” at time 0, before drifting off to infinity. The first expression below for R is not hard to check, and the remaining two can be found in (Beyer, 1981, p. 408):

$$\begin{aligned} R &= \sum_{k=0}^{\infty} \binom{2k}{k}^2 (1/5)^{2k} \\ &= \int_0^1 \int_0^1 \frac{1}{1 - (2/5) \cos(\pi x) - (2/5) \cos(\pi y)} dx dy \\ &= (2/\pi)K(4/5) \end{aligned}$$

with $K(k)$ denoting Legendre’s complete elliptic integral of the first kind. The expected number of steps to create the random spanning tree is bounded by $R \doteq 1.27025$ times the number of vertices, and the remaining steps are readily done deterministically in linear time.

5. Height Functions and Winding Numbers

In this section we describe the connection between the winding number of a spanning tree on a planar graph G and a *height function* on its corresponding matching graph \mathcal{H} . The result, Theorem 3 below, answers a question posed to the first author by Itai Benjamini.

5.1. Height function definition

We assume that G is connected and that $\mathcal{H}(G)$ is embedded in the plane with straight edges. The straight-line embedding is not necessary for the definition (see below) but the construction is more geometric in this case. Moreover, we assume that $\mathcal{H}(G)$ is embedded so that one of f^* or v^* is the outer node (as in Figure 7), or else both f^* and v^* are on the outer facet (as in Figure 8).

Recall that each facet of $\mathcal{H}(G)$ is a quadrilateral containing a node \bar{v} , a node \bar{f} , and two nodes \bar{e}_1, \bar{e}_2 . The nodes \bar{v} and \bar{f} are opposite each other. Let d be the diagonal of the quadrilateral facet directed from \bar{v} to \bar{f} . Let $\arg(d) \in [0, 2\pi)$ denote the angle of the vector d with respect to the x -axis.

Let M be a perfect matching of $\mathcal{H}(v^*, f^*)$ and T, T^\perp respectively the associated spanning tree and its dual. Let \mathbb{D} be the set of the diagonals of facets of $\mathcal{H}(G)$. We will define a real-valued **height function** $h: \mathbb{D} \rightarrow \mathbb{R}$ associated with matching M (refer to Figure 7 and Figure 8).

Remark In many of our examples in § 6, one or more vertex or face nodes are drawn in an extended format. In these cases, the “diagonals” incident to an extended node may

be drawn from any point in the node. In many situations it is natural to draw more than one diagonal on a facet if one of the nodes bounding it is drawn in an extended fashion (as in Figure 8), and then each of the diagonals gets its own height. For instance, to recover the standard definition of height function for matchings of subgraphs of \mathbb{Z}^2 , it is necessary to draw multiple diagonals (see Figure 8). It is thus more natural to view the heights as being defined on the diagonals of the facets rather than the facets themselves.

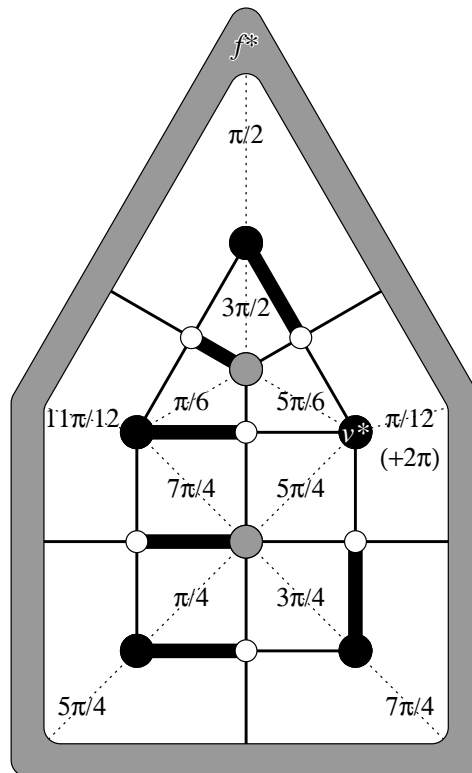


Figure 7: The height function for the perfect matching in Figure 1. Since v^* and f^* are unmatched, the height drops by 2π on the facet containing v^* and f^* .

We first cut the plane along the links in the perfect matching M . We need every vertex-node and face-node to be at the end of one cut, and since neither v^* nor f^* is in the matching M , we make one additional cut, from v^* to f^* . If both v^* and f^* border the outer facet, then we make the cut between them pass through ∞ . If one of v^* or f^* is the outer node, then we view the outer node as being at ∞ , so that the cut still goes to ∞ . It is convenient to make this cut split the diagonal from v^* to f^* , so that there are two diagonals in \mathbb{D} from v^* to f^* , one on either side of the cut.

We require the height function h to satisfy the following local constraint. Suppose d and d' are two diagonals that share a vertex node or face node x . Let θ be the angle required to rotate d to d' around x . Either the counterclockwise (positive) rotation or

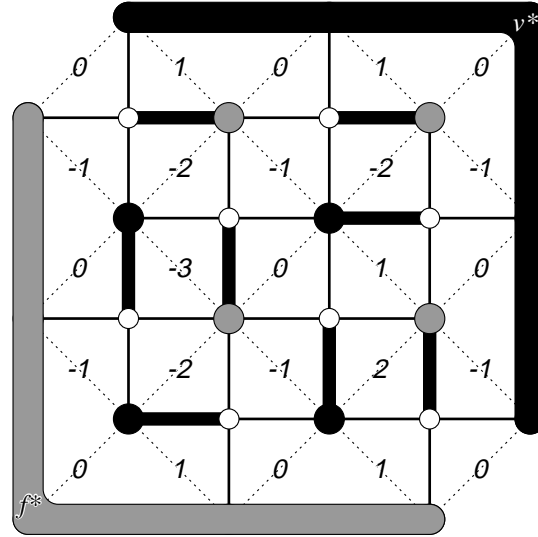


Figure 8: The height function associated with a perfect matching of another graph. For backwards compatibility with previous definitions of the height function associated with dimers on the square lattice, we have (1) measured the heights in quarter-turns rather than in radians, which introduces a scale factor of $\pi/2$, and (2) drawn multiple diagonals (each with its own height) on facets bounded by an extended node.

the clockwise (negative) rotation will encounter the cut containing x ; we take θ to be the rotation which avoids the cut. The local constraint is

$$h(d') = h(d) + \theta.$$

Lemma 2 *Up to a global additive constant, there is a unique height function which satisfies the local constraints. The additive constant can be chosen so that for each diagonal d , $h(d) \equiv \arg(d) \pmod{2\pi}$.*

PROOF: If two diagonals share the same vertex node or face node, then their height difference is determined by the local constraints. Suppose that vertices v_1 and v_2 of G are connected by an edge, and that f is a face bounded by this edge. The height difference between the diagonal from v_1 to f and the diagonal from v_2 to f is determined, and consequently, the local constraints determine the height difference between any diagonal with v_1 as vertex node and any other diagonal with v_2 as vertex node. Since G is connected, there can be at most one height function (up to global additive constant).

We next check that the local constraints do not overconstrain the height function, i.e. that there is a height function satisfying them. Between any two diagonals for which there is a local constraint, one can draw a path connecting the diagonals but which avoids the cuts. If the local constraints were inconsistent, then there would be a closed loop in the plane, which avoids the cuts, such that the local constraints on the diagonals crossed by the loop are inconsistent. Since the cut from v^* to f^* passes through ∞ , the interior of this loop does not contain v^* or f^* . Consider such a contradictory loop surrounding a minimal number of links in the matching M . The loop must cross at least one diagonal between a vertex node and a face node, and one of these nodes must be in the interior of the loop. Call this node x . Since x is not v^* or f^* , it is paired with an edge node y in the matching. Since the loop avoids cuts, y is also in the interior of the loop.

Since x is a vertex node or a face node, the local constraints on the diagonals incident to x involve rotations that avoid the cut from x to y , and they are evidently consistent. Since y is an edge node, there are four facets of $\mathcal{H}(G)$ incident to y , and the four diagonals in these facets form a quadrilateral containing y . The total height change going *clockwise* around y is then the sum of the interior angles of this quadrilateral, excluding the angle at the node x . Since the sum of the interior angles of a quadrilateral is 2π , the total height change around y is 2π minus the angle at x . Thus the total height change going around the cut from x to y is constrained to be zero. Therefore the contradictory loop can be deformed to exclude x and y from its interior, contradicting our assumption that it surrounds a minimal number of links from the matching M . We conclude that there are no such contradictory loops, and that the height function is well-defined (up to a global additive constant).

The second statement of the lemma follows by noting that if for some diagonal d , $h(d) \equiv \arg(d) \pmod{2\pi}$, then this relation holds for the neighboring diagonals as well. \square

Note that in the case of a matching of \mathbb{Z}^2 , this definition of height function is $2\pi/4$ times the standard definition due to Thurston (1990) (see Figure 8). It is also essentially equivalent to, but more geometrical than, the definition due to Propp (1993).

When $\mathcal{H}(G)$ is embedded in the plane but not with straight edges, one can still assign to each diagonal d an angle which is the argument of the vector representing the difference in its endpoints. The orientation of the triple d, ℓ, d' is a topological condition

and so does not depend on the fact that the edges of $\mathcal{H}(G)$ are straight. Thus it is possible to define the height for any embedding of $\mathcal{H}(G)$.

5.2. Turning and heights

Let γ be a simple path (in topological terms, a “directed arc”) in the spanning tree T from v' to v'' ; specifically γ is the link path

$$v' = v_0, e_0, v_1, e_1, \dots, v_{r-1}, e_{r-1}, v_r = v''.$$

Note that the matching of $\mathcal{H}(v^*, f^*)$ that corresponds to T matches node v_i with node e_i for all $0 \leq i \leq r-1$. Let e_r be an edge-node (adjacent to v_r) towards which the path can be continued.

Let f_1, \dots, f_k be the chain of facets of $\mathcal{H}(G)$ which share a node with γ and lie to the left of γ , where f_1 contains the first link v_0e_0 and f_k contains the link $e_{r-1}v_r$. Then for $i \in [1, k-1]$ the facets f_i and f_{i+1} are adjacent along a single link of $\mathcal{H}(G)$, which furthermore is an *unmatched* link (this is a link which shares a node with γ but is not in γ ; therefore it is unmatched).

The *winding number* of γ is defined to be the total angle of the left turns minus the total angle of right turns, from v_0 to v_r (the “initial” angle of γ is the direction of v_0e_0 and the “final” angle of γ is the direction of v_re_r).

Theorem 3 *The winding number of γ is equal to $(h(f_k) - c_k) - (h(f_1) - c_1)$, where c_1 is the counterclockwise angle from the vector v_0e_0 to the diagonal d_1 , and c_k is the counterclockwise angle from the vector v_re_r to the diagonal d_k .*

Here we may view the heights as being defined on the facets, since even if facet f_j has more than one diagonal, $h(f_j) - c_j$ has the same value no matter which diagonal is used.

PROOF OF THEOREM: Without loss of generality we may assume that the height at facet f_1 is $h(f_1) = \arg(d_1)$. Then $h(f_1) - c_1$ is the angle that the initial direction of γ makes with the x -axis. Let f_j be a facet adjacent to v_ℓ . Then similarly $h(f_j) - c_j$ is equal modulo 2π to the angle that $v_\ell e_\ell$ makes with the x -axis.

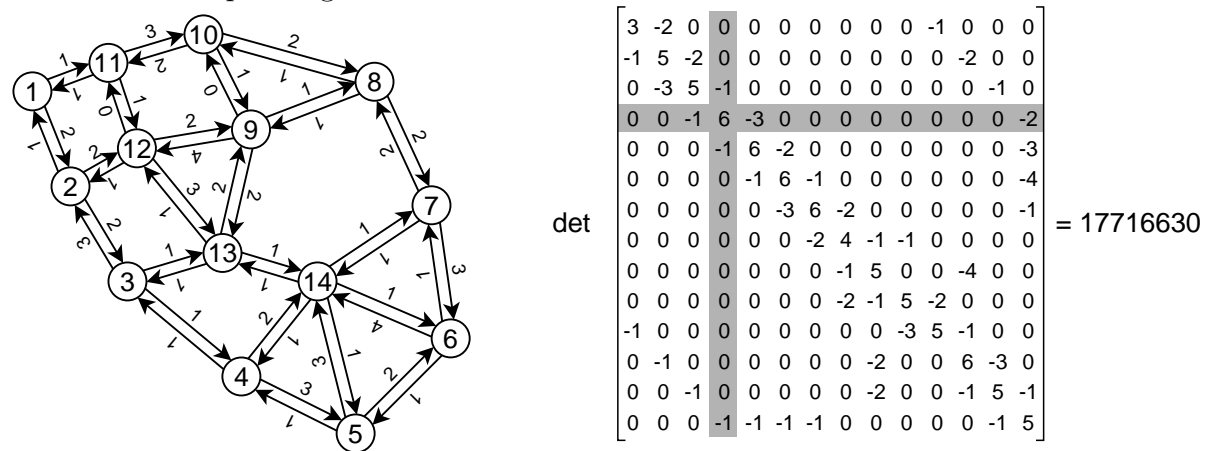
If f_j is the last facet adjacent to v_ℓ , so that f_{j+1} is adjacent to $v_{\ell+1}$, then the difference $(h(f_{j+1}) - c_{j+1}) - (h(f_j) - c_j)$ equals the increase in angle from $v_j e_j$ to $v_{j+1} e_{j+1}$ (which is negative at a right turn). The proof follows. \square

6. Explicit Formulas

Here we use the generalized Temperley bijection to count perfect matchings of certain finite subgraphs of the infinite square grid and infinite square-octagon grid, making use of spanning trees. The enumeration techniques closely follow the derivation of the exact formula for the number of domino tilings of the $(2n+1) \times (2n+1)$ square with a corner removed; see Lovász (1979) and Propp (1995).

One motivation for some of these calculations is that they can be used to compute asymptotic formulas for the number of dimer configurations on more general regions, via techniques developed in Kenyon (1998). For example, using the exact formula for the triangular or diamond regions in §§6.5–6.8, one should be able to extend the asymptotic formula in Kenyon (1998) to polygonal regions whose boundary edges have slopes in $\{0, 1, -1, \infty\}$. Using the example in 6.9 should give rise to a similar asymptotic formula for regions of the hexagonal lattice. Other formulas corroborate refinements of the entropy formula that predict how the the lower-order asymptotics of the number of spanning trees should reflect the geometry of the boundary of the graph (see Duplantier and David (1988) and Kenyon (1998)).

To enumerate the spanning trees of a graph, we make use of the well-known Matrix Tree Theorem (see e.g. Biggs (1993)), as illustrated below. Given a directed graph G with n vertices, the negative Laplacian of G is the $n \times n$ matrix $L(G)$, where $L(G)_{v,w}$ ($v \neq w$) equals the negative of the weight of the edge from vertex v to vertex w , and $L(G)_{v,v}$ is the weighted sum of the arcs emanating from v . The determinant of the submatrix obtained by deleting row r and column r from $L(G)$ gives the (weighted) number of the spanning trees rooted at r .



extra vertex in a spanning tree in the new graph. (The details are left to the reader.)

Every graph considered in the examples below either is a finite induced subgraph of an infinite square grid or else is obtained from such a graph by adding a single additional vertex. In each case we give an explicit formulas for the eigenfunctions. We hasten to say that for a general planar graph an explicit diagonalization would be much more difficult. The tractability of our chosen examples arises from their connection with the negative Laplacian of the infinite square grid \mathbb{Z}^2 . A function f on \mathbb{Z}^2 is an eigenfunction of the negative Laplacian if it satisfies the equation

$$4f(x, y) - f(x - 1, y) - f(x + 1, y) - f(x, y - 1) - f(x, y + 1) = \lambda f(x, y)$$

for all integers x, y , in which case λ is the associated eigenvalue. For each pair of complex numbers ζ, ζ' satisfying $|\zeta| = |\zeta'| = 1$, we can construct such an eigenfunction by putting $f(x, y) = \zeta^x \zeta'^y$ and $\lambda = 4 - \zeta - \zeta^{-1} - \zeta' - \zeta'^{-1}$. In many cases, the restriction of such a function $f(x, y)$ to points x, y lying in some finite region in \mathbb{Z}^2 is an eigenfunction of the matrix associated with that region by the Matrix Tree Theorem.

As a preparatory example, we briefly mention here the trivial case of counting spanning trees of an undirected chain C consisting of n vertices and $n - 1$ edges. The space of complex-valued functions on the vertices of C can be identified with the n -dimensional space W of odd periodic functions of period $2n + 2$, i.e. functions $f : \mathbb{Z} \mapsto \mathbb{C}$ that satisfy $f(-x) = f(2n + 2 - x) = -f(x)$ for all x in \mathbb{Z} (and that consequently satisfy $f(0) = f(n + 1) = \dots = 0$). Under this identification, the negative Laplacian of C is carried over to the negative Laplacian of \mathbb{Z} , giving rise to an eigenbasis for W of the form $f_k(x) = \sin \frac{kx\pi}{n+1}$ ($1 \leq k \leq n$).

We draw each graph (see Figures 9 through 17) so that the non-root vertices are located at points of the lattice, and so that every edge of the graph connects nearest neighbors in the lattice. With high-degree root vertices it is necessary to draw the root vertex in an extended fashion, covering multiple points of the lattice, to ensure that all the edges incident to the root are drawn between neighboring points in the lattice.

Generally the requisite eigenvectors of the matrix $L(G)$ (either with or without the root row and column deleted) will be eigenvectors of the negative Laplacian of the infinite lattice that also satisfy certain boundary conditions (analogous to the conditions $f(0) = f(n + 1) = 0$ in the preparatory example). Usually the infinite lattice will be \mathbb{Z}^2 although sometimes it will be $(\mathbb{Z} + \frac{1}{2})^2 = \{(x, y) : x - \frac{1}{2}, y - \frac{1}{2} \in \mathbb{Z}\}$. There are two types of boundary conditions. Suppose that v and w are nearest neighbors in the lattice, and v is a non-root vertex of the graph. If w is not in the graph, then we require that $f(v) = f(w)$. If the root vertex is drawn so as to contain the point w , and the root row and column are deleted from $L(G)$, then we require that $f(w) = 0$. We leave it to the reader to check that if f satisfies these boundary conditions, then the restriction of f to G is an eigenvector of the matrix with eigenvalue λ .

For certain subgraphs of the square-octagon graph, exact formulas for the number of perfect matchings can be found by doing urban renewal to get a weighted version of one of the graphs shown below. In each case the eigenvectors of the weighted version can

be obtained from the eigenvectors of the unweighted version by multiplying by weights 2^{i+j} and 2^{-i-j} as in § 4. The eigenvalue in the weighted version is obtained from the unweighted eigenvalue by adding 1.

In the rest of this section we give a number of graphs G , their duals G^\perp , the graphs $\mathcal{H}(v^*, f^*)$, the eigenvectors of $L(G)$ (possibly with root row and column removed), and the corresponding formula for the number of perfect matchings of $\mathcal{H}(v^*, f^*)$. When G is undirected, we can also enumerate the matchings of $\mathcal{H}(v^*, f^*)$ by counting the spanning trees of the dual of G .

6.1. Temperley’s bijection

Temperley’s original bijection involved computing the number of perfect matchings of a $2\ell - 1$ by $2m - 1$ subgraph of the square grid with a corner removed. By the main theorem, this is the number of spanning trees of an $\ell \times m$ rectangle. The eigenvectors

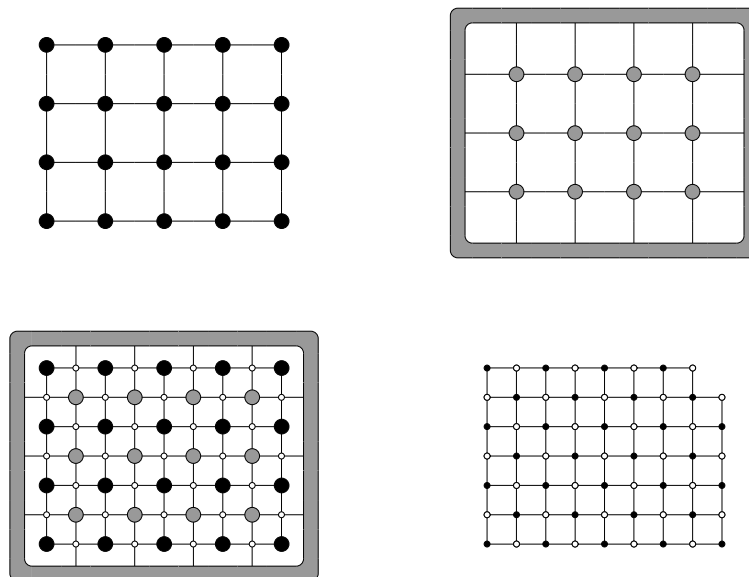


Figure 9: Temperley’s original bijection, for the odd-by-odd rectangular region with a corner removed. $\ell = 5$, $m = 4$.

of the negative Laplacian are of the form

$$f(x, y) = f_{j,k}(x, y) = \cos \frac{\pi j x}{\ell} \cos \frac{\pi k y}{m},$$

where x runs from $\frac{1}{2}$ to $\ell - \frac{1}{2}$ by integer steps and y from $\frac{1}{2}$ to $m - \frac{1}{2}$ by integer steps, j is an integer in $[0, \ell - 1]$ and k is an integer in $[0, m - 1]$. (The lower left vertex is $(x, y) = (\frac{1}{2}, \frac{1}{2})$ and the upper right vertex is $(x, y) = (\ell - \frac{1}{2}, m - \frac{1}{2})$.) The eigenvalue of $f_{j,k}$ is $4 - 2 \cos \frac{\pi j}{\ell} - 2 \cos \frac{\pi k}{m}$, which is zero when $k = \ell = 0$. The number of spanning trees is

$$\frac{1}{\ell m} \prod \left[4 - 2 \cos \frac{\pi j}{\ell} - 2 \cos \frac{\pi k}{m} \right]$$

where the product is taken over all pairs (j, k) with $0 \leq j \leq \ell - 1, 0 \leq k \leq m - 1$ except $(0, 0)$.

Using panel (b) of Figure 9, we can compute the number of spanning trees in a different way. In this case we take the negative Laplacian of the graph in panel (b) and remove a row and column corresponding to the outer vertex. The eigenvectors of the resulting graph are as follows.

$$f_{j,k}(x, y) = \sin \frac{\pi j x}{\ell} \sin \frac{\pi k y}{m},$$

where this time x runs from 0 to ℓ by integer steps and y from 0 to m by integer steps, j is an integer in $[1, \ell - 1]$ and k an integer in $[1, m - 1]$. Note that the x, y coordinates correspond to the centers of the faces in the coordinates of panel (a). The corresponding eigenvalue is $4 - 2 \cos \frac{\pi j}{\ell} - 2 \cos \frac{\pi k}{m}$. The number of spanning trees is

$$\prod_{j=1}^{\ell-1} \prod_{k=1}^{m-1} \left[4 - 2 \cos \frac{\pi j}{\ell} - 2 \cos \frac{\pi k}{m} \right].$$

In this case there is no zero eigenvalue since we have removed a row and column of the negative Laplacian. The equivalence of these two formulas follows from the well-known identity for $\ell = \prod_{j=1}^{\ell-1} (2 - 2 \cos \frac{\pi j}{\ell})$.

6.2. Dimers on an even-by-odd rectangle

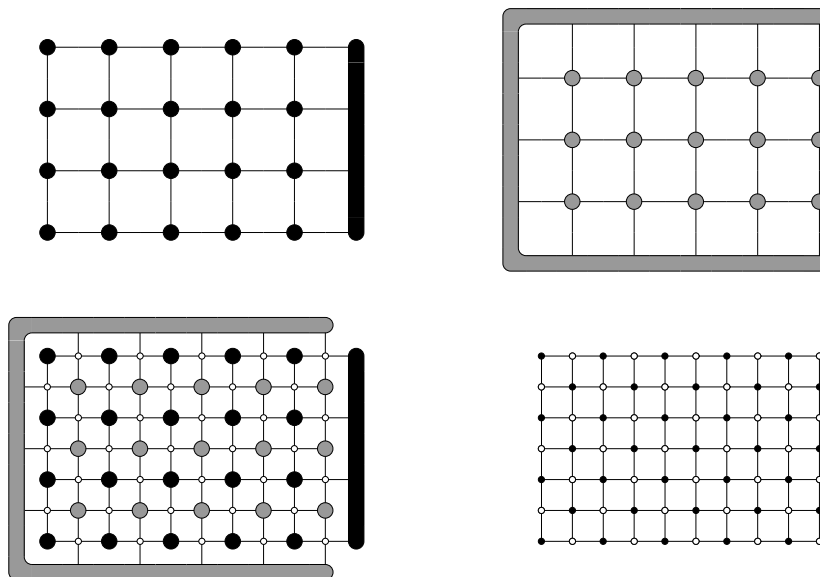


Figure 10: The even-by-odd rectangular region. $\ell = 5, m = 4$.

See Figure 10. In this case we again remove the row and column from the negative Laplacian corresponding to the “extended” vertex. The eigenvectors of the negative

Laplacian are of the form

$$f_{j,k}(x, y) = \cos \frac{\pi(2j + 1)x}{2\ell + 1} \cos \frac{\pi ky}{m},$$

where x runs from $\frac{1}{2}$ to $\ell + \frac{1}{2}$ and y from $\frac{1}{2}$ to $m - \frac{1}{2}$, j is an integer in $[0, \ell - 1]$ and k is an integer in $[0, m - 1]$. The corresponding eigenvalue is $4 - 2 \cos \frac{\pi(2j+1)}{2\ell+1} - 2 \cos \frac{\pi k}{m}$. The number of spanning trees is

$$\prod_{j=0}^{\ell-1} \prod_{k=0}^{m-1} \left[4 - 2 \cos \frac{\pi(2j + 1)}{2\ell + 1} - 2 \cos \frac{\pi k}{m} \right].$$

Similarly, in panel (b) with the extended vertex removed the eigenvectors are

$$f_{j,k}(x, y) = \sin \frac{\pi(2j + 1)x}{2\ell + 1} \sin \frac{\pi ky}{m},$$

where x runs from 0 to ℓ and y from 0 to m , j is an integer in $[0, \ell - 1]$ and k is an integer in $[1, m - 1]$. The corresponding eigenvalue is $4 - 2 \cos \frac{\pi(2j+1)}{2\ell+1} - 2 \cos \frac{\pi k}{m}$.

6.3. Dimers on an even-by-even rectangle

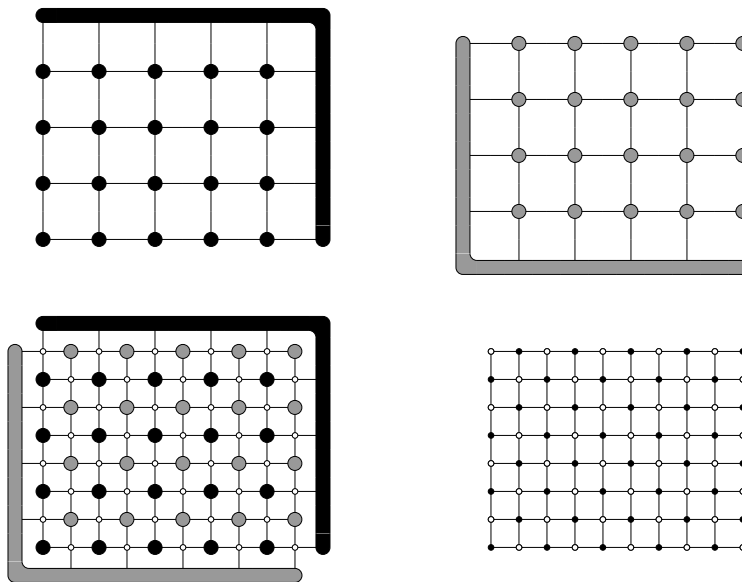


Figure 11: The even-by-even rectangular region. $\ell = 5, m = 4$.

See Figure 11. In panel (a) the eigenvectors of the negative Laplacian after removal of the extended vertex are

$$f_{j,k}(x, y) = \cos \frac{\pi(2j + 1)x}{2\ell + 1} \cos \frac{\pi(2k + 1)y}{2m + 1},$$

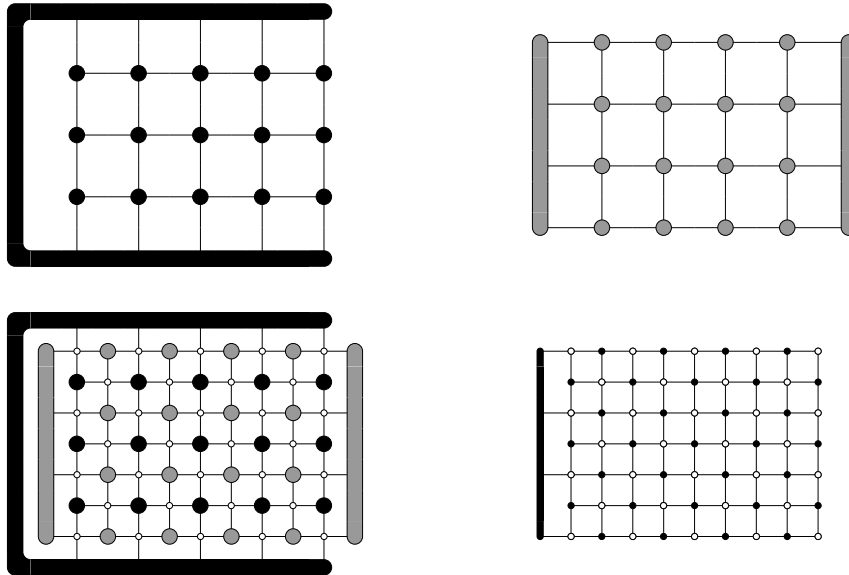


Figure 12: The odd-by-odd rectangular region with an extra vertex connecting every other vertex on the left side. $\ell = 5, m = 4$.

where x runs from $\frac{1}{2}$ to $\ell + \frac{1}{2}$ and y from $\frac{1}{2}$ to $m + \frac{1}{2}$, j is an integer in $[0, \ell - 1]$ and k is an integer in $[0, m - 1]$. The number of spanning trees is

$$\prod_{j=0}^{\ell-1} \prod_{k=0}^{m-1} \left[4 - 2 \cos \frac{\pi(2j+1)}{2\ell+1} - 2 \cos \frac{\pi(2k+1)}{2m+1} \right].$$

For eigenvectors in panel (b) replace the cosines with sines, the x range to 0 to ℓ , and the y range 0 to m . The formula for the determinant is identical.

6.4. Dimers on an odd-by-odd rectangle with an extra vertex

See Figure 12. In panel (a) the eigenvectors of the negative Laplacian after removal of the extended vertex are

$$f_{j,k}(x, y) = \cos \frac{\pi j x}{\ell} \sin \frac{\pi k y}{m},$$

where x runs from $\frac{1}{2}$ to $\ell - \frac{1}{2}$ and y from 0 to m , j is an integer in $[0, \ell - 1]$ and k is an integer in $[1, m - 1]$. The number of spanning trees is

$$\prod_{j=0}^{\ell-1} \prod_{k=1}^{m-1} \left[4 - 2 \cos \frac{\pi j}{\ell} - 2 \cos \frac{\pi k}{m} \right].$$

The eigenvectors in panel (b) are more complicated.

Remark The formula for this region can also be derived by multiplying m (the number of ways the extra vertex can be paired) by Temperley's formula for the odd-by-odd

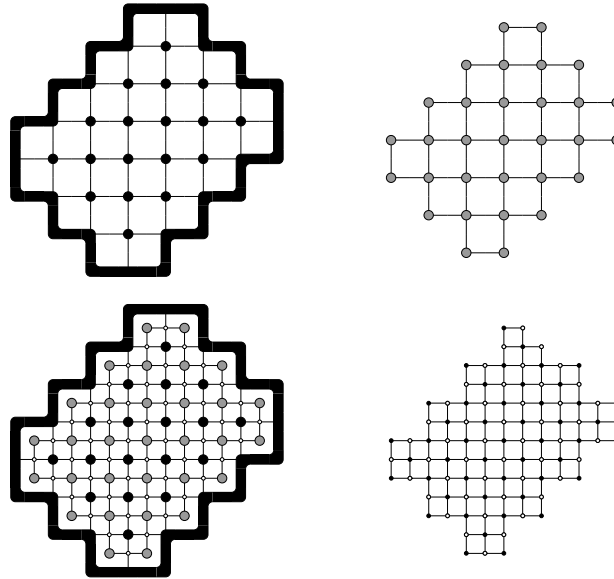


Figure 13: A diamond-shaped region with $\ell = 4, m = 3$.

region with a corner removed, since Temperley's formula still holds with other perimeter vertices of the right parity removed instead of the corner.

6.5. A diamond-shaped region

See Figure 13. In panel (a) the eigenvectors of the negative Laplacian after removal of the extended vertex are

$$f_{j,k}(x, y) = \sin \frac{\pi j(x + y)}{2\ell} \sin \frac{\pi k(x - y)}{2m},$$

where the origin $(x, y) = (0, 0)$ is in the center bottom part of the extended outer vertex of G , $x \in [-m, \ell]$, and $y \in [0, \ell + m]$, with $0 \leq x + y \leq 2\ell$ and $0 \leq y - x \leq 2m$. The indices $(j, k) \in [1, 2\ell - 1] \times [1, m - 1] \cup [1, \ell] \times \{m\}$. The number of spanning trees is

$$\prod_{j,k} \left[4 - 4 \cos \frac{\pi j}{2\ell} \cos \frac{\pi k}{2m} \right],$$

where (j, k) runs over this range.

6.6. Another diamond-shaped region

See Figure 14. In panel (a) the eigenvectors of the negative Laplacian after removal of the extended vertex are

$$f_{j,k}(xy) = \sin \frac{\pi j(x + y)}{2\ell} \sin \frac{\pi k(x - y)}{2m},$$

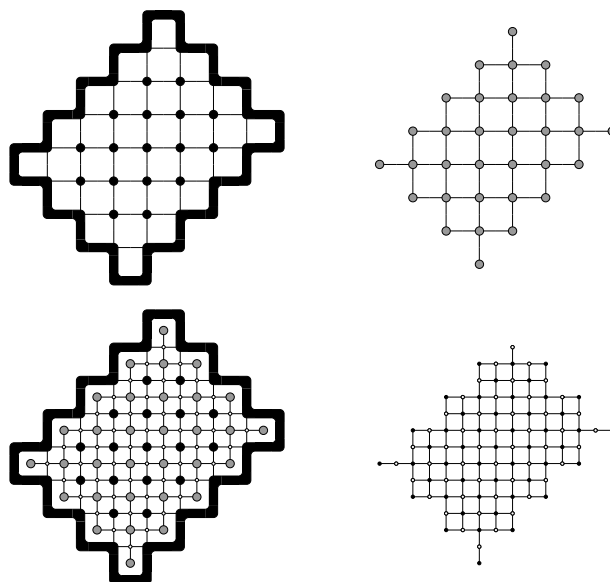


Figure 14: Another diamond-shaped region, with $\ell = 4, m = 3$.

where the origin $(x, y) = (0, 0)$ is at the bottom vertex of G^\perp , $x \in [-m, \ell]$, and $y \in [0, \ell + m]$, with $0 \leq x + y \leq 2\ell$ and $0 \leq y - x \leq 2m$. The indices $(j, k) \in [1, 2\ell - 1] \times [1, m - 1] \cup [1, \ell - 1] \times \{m\}$. The number of spanning trees is

$$\prod_{j,k} \left[4 - 4 \cos \frac{\pi j}{2\ell} \cos \frac{\pi k}{2m} \right],$$

where (j, k) runs over this range. Note that this is exactly the formula of the previous section, except for the index $(j, k) = (\ell, m)$ whose eigenvalue is 4. As a consequence the number of spanning trees of this diamond is exactly one-fourth the number of spanning trees of the previous diamond. This fact was first observed by Stanley (1996) (when $\ell = m$), and was first proved by Knuth (1997) and Ciucu (1998) (without assuming $\ell = m$); a generalization was stated and proved by Chow (1997).

Again we cannot compute the eigenvectors in panel (b).

Similar formulas hold for two additional diamond-shaped regions with boundaries intermediate between those shown in Figures 13 and 14.

6.7. A triangular region

See Figure 15. In panel (a) the eigenvectors of the negative Laplacian after removal of the extended vertex are

$$f_{j,k}(x, y) = \sin \frac{\pi(2j+1)x}{2m+1} \sin \frac{\pi(2k+1)y}{2m+1} - \sin \frac{\pi(2k+1)x}{2m+1} \sin \frac{\pi(2j+1)y}{2m+1},$$

where the origin $(x, y) = (0, 0)$ is the lower-bottom-most part of the extended external vertex, x and y run from 0 to m , with $x \geq y$, and j and k are integers in $[0, m - 1]$ with

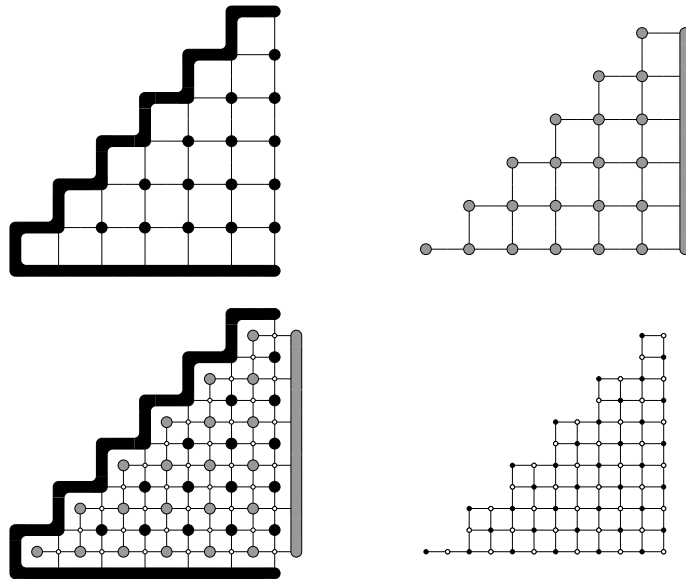


Figure 15: A triangular region. $m = 6$.

$j < k$. The number of spanning trees is

$$\prod_{0 \leq j < k < n} \left[4 - 2 \cos \frac{\pi(2j+1)}{2m+1} - 2 \cos \frac{\pi(2k+1)}{2m+1} \right].$$

We don't know how to compute the eigenvectors of the negative Laplacian of the graph in panel (b).

Remark This family of regions has been studied by Mihai Ciucu and Lior Pachter. Ciucu (1997) showed combinatorially that the number of domino tilings of the $2n \times 2n$ square equals 2^n times the square of the number of domino tilings of a particular region H_n , so one way to prove the claim (not the one given here!) is to hitch a ride on the formula for the number of domino tilings of the square — or you could turn this around and derive the formula for the number of tilings of the square as a corollary of the above formula. Also, Pachter (1997) gave a purely combinatorial proof that the number of domino tilings of H_n is odd. A different way to see this uses 2-adic analysis of the factors in the double product (Cohn, 1999).

6.8. Another triangular region, and the quartered Aztec diamond

See Figure 16.

In panel (a) the eigenvectors of the negative Laplacian after removal of the extended vertex are

$$f_{j,k}(x, y) = \sin \frac{\pi j x}{m} \sin \frac{\pi k y}{m} - \sin \frac{\pi k x}{m} \sin \frac{\pi j y}{m},$$

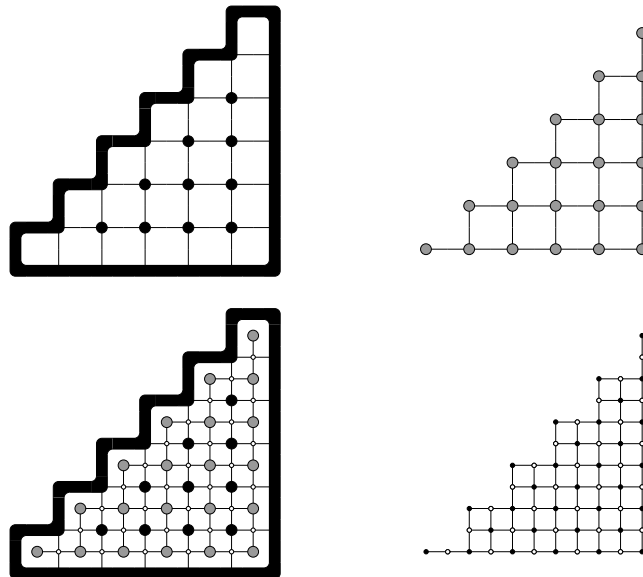


Figure 16: Another triangular region. G^\perp in panel (b) is the “quartered Aztec diamond.” $m = 6$.

where the origin $(x, y) = (0, 0)$ is the lower-bottom-most part of the extended external vertex, x and y run from 0 to m , with $x \geq y$, and j and k are integers in $[1, m - 1]$ with $j < k$. The number of spanning trees is

$$\prod_{0 < j < k < m} \left[4 - 2 \cos \frac{\pi j}{m} - 2 \cos \frac{\pi k}{m} \right].$$

We don’t know how to compute the eigenvectors of the negative Laplacian of the graph in panel (b).

Remark A formula for the number of spanning trees of the “quartered Aztec diamond” (G^\perp here) had been an open problem for some years before Mihai Ciucu found an expression for it (in work that has not yet been written up). Here we effectively get a formula for it by doing Fourier analysis on the dual graph. The equivalence of Ciucu’s formula and ours does not appear to be an effortless identity.

6.9. A subregion of the hexagonal lattice

Let $\omega = e^{2\pi i/3}$ and $\mathbb{Z}[\omega]$ be the lattice of Eisenstein integers. Let G be the directed graph whose vertices are $\mathbb{Z}[\omega]$, each vertex v having an edge directed towards the three vertices $v + 1, v + \omega, v + \omega^{-1}$, as in Figures 2a and 17a.

Here we obtain an exact formula for the number of directed spanning trees on the triangular region T_m in G whose vertices are $0, m, -m\omega^{-1}$, with “wired” boundary conditions (Figure 17).

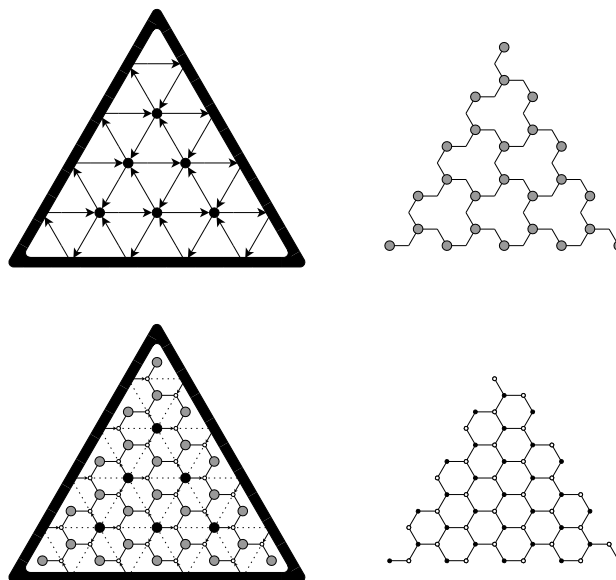


Figure 17: A triangular region of the hexagonal lattice. Here $n = 5$, and $m = n - 2 = 3$.

Let $n = m + 2$. Let Λ_n be the sublattice of $\mathbb{Z}[\omega]$ generated by $n(1 - \omega^{-1})$ and $n(\omega - \omega^{-1})$. A fundamental domain for Λ_n is given by the hexagon whose vertices are $0, n, n(1 - \omega^{-1}), -2n\omega^{-1}, n(\omega - \omega^{-1}), n\omega$. This fundamental domain is tiled with six copies of the equilateral triangle whose vertices are $0, n, -n\omega^{-1}$. The graph T_m is embedded in this triangle as the set of vertices not touching the boundary.

Let $f_{\alpha, \beta, \gamma}$ be the function on $\mathbb{Z}[\omega]$ such that $f_{\alpha, \beta, \gamma}(x + y\omega + z\omega^{-1}) = \alpha^x \beta^y \gamma^z$; single-valuedness implies $\alpha\beta\gamma = 1$. The function $f_{\alpha, \beta, \gamma}$ is an eigenvector of the negative Laplacian of G , and has eigenvalue $3 - \alpha - \beta - \gamma$. In order for $f_{\alpha, \beta, \gamma}$ to be a function on the torus G/Λ_n , the relations $(\alpha/\gamma)^n = 1$ and $(\beta/\gamma)^n = 1$ must also hold. If α is a $3n$ th root of unity, and α/γ is an n th root of unity, then $\beta/\gamma = 1/(\alpha\gamma^2)$ is also an n th root of unity, so that $f_{\alpha, \beta, \gamma}$ is an eigenvector of the torus G/Λ_n with eigenvalue $3 - \alpha - \beta - \gamma$. The various $f_{\alpha, \beta, \gamma}$'s formed in this way are orthogonal on the torus, and since there are $3n^2$ of them, the same as the number of vertices in the torus, they form an eigenbasis of the negative Laplacian of the torus.

Let L_1, L_2, L_3 be the three lines of symmetry of the lattice $\mathbb{Z}[w]$ defined by $L_1 = \mathbb{R}$, $L_2 = \omega\mathbb{R}$, and $L_3 = \omega^{-1}\mathbb{R}$. Orthogonal reflection in each of these lines is not only a symmetry of the lattice but preserves Λ_n and the edge directions. Therefore these reflections are symmetries of the underlying graph on the torus. The lines L_1, L_2, L_3 project to the torus, cutting it into 6 equilateral triangles. Say that a function on the torus is skew symmetric if reflecting it through any of the lines L_1, L_2, L_3 is equivalent to negating the function. Since reflection in a line of symmetry L_1, L_2 , or L_3 sends the eigenvector $f_{\alpha, \beta, \gamma}$ on the torus to the eigenvector $f_{\alpha, \gamma, \beta}$, $f_{\gamma, \beta, \alpha}$, or $f_{\beta, \alpha, \gamma}$ respectively (in each case two subscripts have been transposed), when we express any skew symmetric function as a linear combination of the $f_{\alpha, \gamma, \beta}$'s, we find that it is a linear combination of

the $g_{\alpha,\gamma,\beta}$'s, which are defined by

$$g_{\alpha,\beta,\gamma} = \sum_{\sigma \in S_3} (-1)^\sigma f_{\sigma(\alpha,\beta,\gamma)} = f_{\alpha,\beta,\gamma} - f_{\alpha,\gamma,\beta} + f_{\gamma,\alpha,\beta} - f_{\gamma,\beta,\alpha} + f_{\beta,\gamma,\alpha} - f_{\beta,\alpha,\gamma}.$$

$g_{\alpha,\beta,\gamma}$ is an eigenvector of the torus G/Λ_n with eigenvalue $3 - \alpha - \beta - \gamma$. If we restrict our attention to triples (α, β, γ) satisfying $\alpha < \beta < \gamma$ under some arbitrary ordering of the roots of unity, then the $g_{\alpha,\beta,\gamma}$'s still span the space of skew symmetric functions; furthermore a nontrivial linear relation among them would imply a nontrivial linear relation among the $f_{\alpha,\beta,\gamma}$'s, so the $g_{\alpha,\beta,\gamma}$'s such that $\alpha < \beta < \gamma$ form an eigenbasis of the space of skew symmetric functions.

Since the $g_{\alpha,\beta,\gamma}$'s are zero on the lines of symmetry L_1, L_2, L_3 , when we restrict the $g_{\alpha,\beta,\gamma}$'s to one of the 6 equilateral triangles, they form an eigenbasis of the matrix obtained from the negative Laplacian of the triangular subgraph by deleting the vertices on the boundary. Thus multiplying their eigenvalues gives the number of spanning trees of the triangular region with wired boundary conditions, rooted at the wired boundary:

$$\prod_{\substack{\alpha,\beta,\gamma \\ \alpha\beta\gamma=1 \\ \alpha^{3n}=1 \\ (\alpha/\beta)^n=1 \\ \alpha,\beta,\gamma \text{ distinct}}} (3 - \alpha - \beta - \gamma)^{1/6}.$$

The prime factors of the numbers given by this formula exhibit some rather nice patterns.

7. Open Problems

Our work suggests (or might be useful in the solution of) a number of different problems.

First, there is the natural question of extending the correspondence between spanning trees and matchings so that it applies to matchings of more general planar graphs (or perhaps even some non-planar ones). An intriguing example is the "12-6-4 lattice" (the infinite graph obtained by taking the 1-skeleton of the Archimedean tiling of the plane by dodecagons, hexagons, and squares) shown in Figure 18. In a matching, each vertex is paired to another vertex via one of three types of edges: a 6/4 edge (bordering a hexagon and square), a 12/4 edge (bordering a dodecagon and square), or a 12/6 edge (bordering a dodecagon and hexagon). In random perfect matchings of suitably defined subgraphs (chosen so as to minimize the effect of the boundary), the probabilities of these three events are respectively $1/6 + (19/78)R$, $1/3 + (1/39)R$, and $1/2 - (7/26)R$, where R is given by

$$R = \sum_{n=0}^{\infty} \sum_{k=0}^n \binom{2n}{n} \binom{n}{k}^2 \frac{14^k}{13^{2n}}.$$

Curiously, these probabilities also turn up in the random spanning trees of a certain directed weighted cartesian lattice. In this lattice each leftward edge has weight 25, each

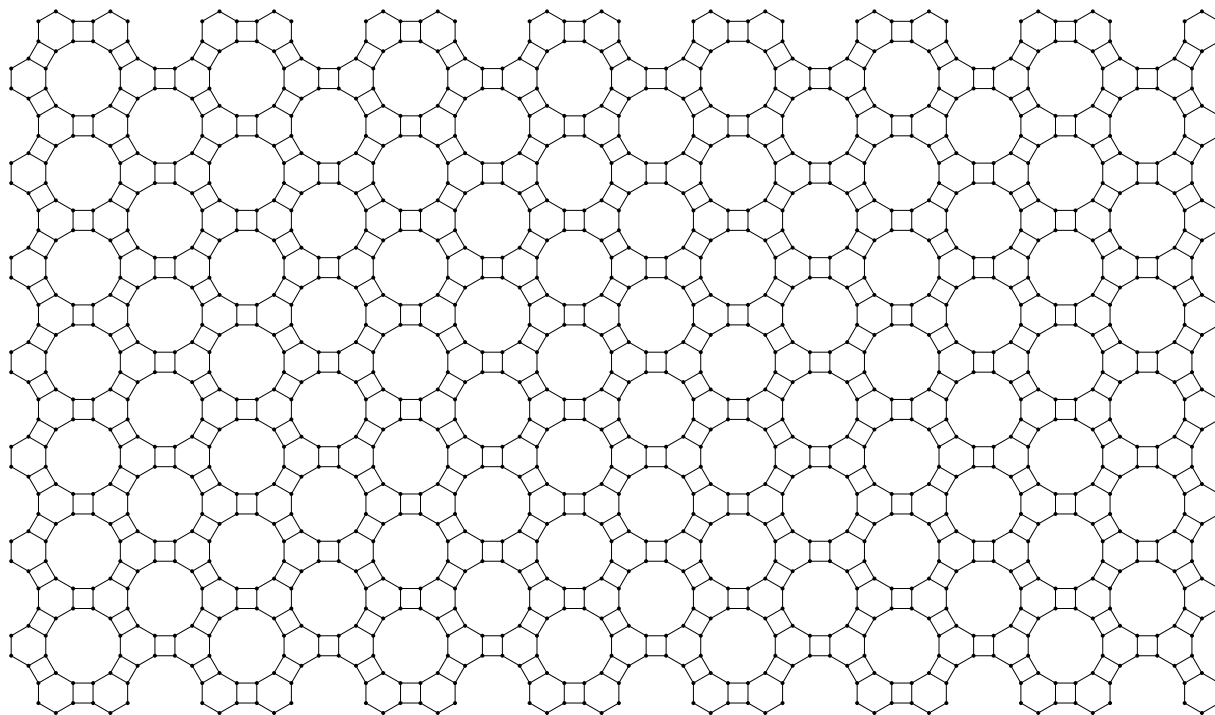


Figure 18: A portion of the “12-6-4 lattice” of dodecagons, hexagons, and squares.

upward edge has weight 25, each rightward edge has weight 14, and each downward edge has weight 1. The probability that in the tree the parent of a vertex is to the left is the same as the probability of a 12/4 edge in the 12-6-4 lattice, and the probability that the parent is above the given vertex is the same as the probability of a 6/4 edge in the 12-6-4 lattice. These “coincidences” suggest a weighted bijective correspondence analogous to the one for the lattice of octagons and squares, but we have been unable to find one.

One side-issue of a number-theoretic nature concerns the formula given at the end of § 6.9. As was mentioned, there are some interesting patterns governing the prime factors of these numbers; for instance, it appears that most of the large prime factors, including the very largest, are congruent to 1 mod n . It would be good to know why this is true.

Turning to entropy, it would also be desirable to have a more general understanding of asymptotics. In all the examples considered in § 6, the logarithm of the number of spanning trees, divided by the size of the system, tends to a single limit that is independent of the shape of the boundary, but is a numerical characteristic of the infinite square grid. One might ask the same question for more general grids. For example, suppose we have some locally finite infinite planar graph G that admits an adjacency-preserving action of \mathbb{Z}^2 that has only finitely many vertex-orbits and edge-orbits. What is the limit of the normalized logarithm of the number of spanning trees of large finite subgraphs of G , as the subgraphs grow to fill G ? It is not too hard to guess the shape of the answer, using the spectrum of the negative Laplacian, but justifying this answer

would require some care.

There is also the issue of uniqueness of the measure of maximum entropy. In the case of the square grid, Burton and Pemantle (1993) proved that there is a unique translation-invariant measure on spanning trees of the infinite square grid that achieves the entropy bound. This yields an analogous result on domino tilings of the plane. It is natural to ask the question for lozenge tilings of the plane; by the theorems of this article, this is closely related to the problem of determining whether there is a unique measure of maximum entropy for directed spanning trees in the directed triangular lattice.

The Ising partition function and the number of spanning trees of a graph are both evaluations of the Tutte polynomial of the graph at special points; see Welsh (1993) for background on the Tutte polynomial. Evaluating the Tutte polynomial at most points is #P-complete, but at special points the polynomial can be evaluated in polynomial time. For planar graphs these special points include the values for the Ising partition function and the number of spanning trees. For planar graphs there are bijective connections between Ising systems and perfect matchings (Fisher, 1966), and between spanning trees and perfect matchings. Thus it is natural to search for connections between perfect matchings and the other special points of the Tutte polynomial.

Acknowledgements

Part of this research was done while the first author was visiting Microsoft Research. The second author thanks Noam Elkies, Sergey Fomin, and Greg Kuperberg for useful conversations on the topic.

References

- Martin Aigner and Günter M. Ziegler. *Proofs from The Book*. Springer, 1998.
- William H. Beyer, editor. *CRC Standard Mathematical Tables*. CRC Press, 26th edition, 1981.
- Norman Biggs. *Algebraic Graph Theory*. Cambridge Univ. Press, 2nd edition, 1993.
- Robert Burton and Robin Pemantle. Local characteristics, entropy and limit theorems for spanning trees and domino tilings via transfer-impedances. *Annals of Probability*, 21(3):1329–1371, 1993.
- Timothy Y. Chow. The Q -spectrum and spanning trees of tensor products of bipartite graphs. *Proceedings of the American Mathematical Society*, 125(11):3155–3161, 1997.
- Mihai Ciucu. Enumeration of perfect matchings of graphs with reflective symmetry. *Journal of Combinatorial Theory, Series A*, 77:67–97, 1997.
- Mihai Ciucu. A complementation theorem for perfect matchings of graphs having a cellular completion. *Journal of Combinatorial Theory, Series A*, 81:34–68, 1998.

- Henry Cohn. 2-adic behavior of numbers of domino tilings. *Electronic Journal of Combinatorics*, 6(1), 1999. Paper #R14.
- Henry Cohn, Richard Kenyon, and James Propp. A variational principle for domino tilings, 1998. Preprint.
- Bertrand Duplantier and François David. Exact partition functions and correlation functions of multiple Hamiltonian walks on the Manhattan lattice. *Journal of Statistical Physics*, 51(3–4):327–434, 1988.
- Michael E. Fisher. On the dimer solution of planar Ising models. *Journal of Mathematical Physics*, 7(10):1776–1781, 1966.
- Ira M. Gessel and X. G. Viennot. Determinants, paths, and plane partitions, 1989. Preprint.
- Richard Kenyon. Conformal invariance of domino tiling. *The Annals of Probability*, 1997a. To appear.
- Richard Kenyon. Local statistics of lattice dimers. *Annales de l'Institut Henri Poincaré – Probabilités et Statistiques*, 33(5):591–618, 1997b. <http://topo.math.u-psud.fr/~kenyon/match.ps.Z>.
- Richard Kenyon. The asymptotic determinant of the discrete Laplacian. *Acta Mathematica*, 1998. To appear.
- Donald E. Knuth. Aztec diamonds, checkerboard graphs, and spanning trees. *Journal of Algebraic Combinatorics*, 6(3):253–257, 1997.
- Greg Kuperberg. Symmetries of plane partitions and the permanent-determinant method. *Journal of Combinatorial Theory, Series A*, 68:115–151, 1994.
- Bernt Lindström. On the vector representations of induced matroids. *Bulletin of the London Mathematical Society*, 5:85–90, 1973.
- László Lovász. *Combinatorial Problems and Exercises*. North-Holland, 1979.
- Lior Pachter. Combinatorial approaches and conjectures for 2-divisibility problems concerning domino tilings of polyominoes. *Electronic Journal of Combinatorics*, 4(1), 1997. R29.
- James Propp. Lattice structure for orientations of graphs, October 1, 1993. Available from the author.
- James Propp. Dimers and dominoes, March 5, 1995. Available from the author.

- James G. Propp and David B. Wilson. How to get a perfectly random sample from a generic Markov chain and generate a random spanning tree of a directed graph. *Journal of Algorithms*, 27:170–217, 1998.
- Richard Stanley. Problem 251: Spanning trees of Aztec diamonds. *Discrete Mathematics*, 157:383–385, 1996.
- H. N. V. Temperley. In *Combinatorics: Being the Proceedings of the Conference on Combinatorial Mathematics held at the Mathematical Institute, Oxford*, pages 356–357, 1972.
- H. N. V. Temperley. In *Combinatorics: Proceedings of the British Combinatorial Conference 1973*, pages 202–204, 1974. London Mathematical Society Lecture Notes Series #13.
- William Thurston. Conway’s tiling groups. *American Mathematical Monthly*, 97:757–773, 1990.
- Dominic J. A. Welsh. *Complexity: Knots, Colourings and Counting*. London Mathematical Society Lecture Note, #186. Cambridge University Press, 1993.